Spin-Glass Transition of the Three-Dimensional Heisenberg Spin Glass

I. Campos,[1] M. Cotallo-Aban,[2,1] V. Martin-Mayor,[3,1] S. Perez-Gaviro,[2,1] and A. Tarancon[2,1]

[1]*Instituto de Biocomputación y Física de Sistemas Complejos (BIFI), Corona de Aragón 42, Zaragoza 50009, Spain*
[2]*Departamento de Física Teórica, Universidad de Zaragoza, Zaragoza 50009, Spain*
[3]*Departamento de Física Teórica I, Facultad de Ciencias Físicas, Universidad Complutense, 28040 Madrid, Spain*
(Received 22 May 2006; published 20 November 2006)

It is shown, by means of Monte Carlo simulation and finite size scaling analysis, that the Heisenberg spin glass undergoes a finite-temperature phase transition in three dimensions. There is a single critical temperature, at which both a spin glass and a chiral glass ordering develop. The Monte Carlo algorithm, adapted from lattice gauge theory simulations, makes it possible to thermalize lattices of size $L = 32$, larger than in any previous spin-glass simulation in three dimensions. High accuracy is reached thanks to the use of the Marenostrum supercomputer. The large range of system sizes studied allows us to consider scaling corrections.

Recently, decisive evidence for a spin-glass transition [1] in three-dimensional Ising spin glasses was found by us [2] and by Palassini and Caracciolo [3]. These works demonstrated the applicability to spin glasses of our approach [4,5] to finite size scaling (FSS) at the critical temperature, as well as that of Caracciolo and co-workers [6] for the paramagnetic state (see also [7,8]).

However, the situation is still confusing for *Heisenberg* spin glasses [9–17], which is the more experimentally interesting case (see, e.g., [18,19]). Indeed, numerical studies are the only theoretical tool to achieve progress in three dimensions. Early simulations [9] could not reach low enough temperatures due to the dramatic dynamical arrest of the algorithms available at the time, and concluded that the critical temperature, T_c, was strictly zero. Yet, recent studies at lower temperatures [16,17] found indirect indications of a spin-glass transition for Heisenberg spin glasses. Matters are further complicated by the Mauger *et al.* [12] suggestion of a low temperature chiral glass phase, with an Ising-like ordering due to the handedness of the noncollinear spin structures (see definitions below). The simulations of Kawamura and co-workers [13,14] gave ample support to this spin-chirality decoupling scenario (i.e., $T_c = 0$ for the spin glass, but $T_c > 0$ for the chiral glass ordering).

In order to clarify the situation for Heisenberg and *XY* spin glasses in $D = 3$, Young and Lee [15] have recently tried our FSS methods at T_c [2,4]. Although parallel tempering only allowed them [15] to thermalize systems of size up to $L = 12$, very clear results were reached for the *XY* spin glasses. The finite-lattice correlation length [20], ξ_L, was analyzed for several system sizes L. As expected [2,4,5], the dimensionless ratio ξ_L/L crosses neatly at the *same* T_c, for the chiral glass and the spin-glass ordering, for *XY* spin glasses. In the more important case of Heisenberg spin glasses, their results, although inconclusive, were interpreted also as lack of spin-chirality decoupling. This conclusion has been criticized by Kawamura and

Hukushima [14], that studied somehow larger systems on *very* few samples.

Here we show that a finite-temperature spin-glass transition occurs for the Heisenberg spin glass in $D = 3$. The critical temperature for the spin-glass transition coincides with that of the chiral glass. Our results rely on Monte Carlo simulation and FSS analysis at T_c [2,4,5]. We adapt a lattice gauge theory algorithm [21] to our problem. Our algorithm thermalizes $L = 32$ systems, well beyond any previous spin-glass simulation in $D = 3$. The use of Marenostrum, one of the world's largest computing facilities, during (the equivalent of) 2.6×10^4 Pentium IV computing days allowed us to simulate 4000 samples. The phase transition seems to be of the Kosterlitz-Thouless type [22], although we may not exclude a lower critical dimension barely smaller than 3.

We consider the Edwards-Anderson model. The Heisenberg spins $\vec{S}_i = (S_i^x, S_i^y, S_i^z)$, $\vec{S}_i \cdot \vec{S}_i = 1$, live on the nodes a cubic lattice of size L, with periodic boundary conditions. Spins interact via the Hamiltonian ($\langle ij \rangle$ indicates sum over all pairs of lattice nearest neighbors):

$$H = -\sum_{\langle i,j \rangle} J_{ij} \vec{S}_i \cdot \vec{S}_j. \tag{1}$$

The J_{ij} are Gaussian distributed quenched random couplings [1]. Their mean value is zero, while their variance sets the energy unit. For any quantity, O, we first calculate the thermal average for the given couplings, $\langle O \rangle_J$. The average over the J_{ij}, $\overline{\langle O \rangle_J}$, is only taken afterward.

In order to detect nonplanar spin structures, one forms the chiral (pseudovector) density field [13]:

$$\zeta_{i\mu} = \vec{S}_{i+\hat{e}_\mu} \cdot (\vec{S}_i \times \vec{S}_{i-\hat{e}_\mu}) \quad (\mu = x, y, z), \tag{2}$$

where $\hat{e}_\mu$ is the unit lattice vector along the μ axis.

We introduce real replicas [1]: pairs of spin configurations, $\vec{S}_i^{(1)}$ and $\vec{S}_i^{(2)}$ independently evolving with the same set of couplings, $\{J_{ij}\}$, and at the same temperature, T. We

have as well a replicated field for the chiral densities, (2). From the real replicas we form the tensor field $q_{\mu\nu}(\vec{r}_i)$ and the chiral vector field $\kappa_{i,\mu}$: ($\mu, \nu = x, y, z$)

$$q_{\mu,\nu}(\vec{r}_i) = S_{i,\mu}^{(1)} S_{i,\nu}^{(2)}, \qquad \kappa_{i,\mu} = \zeta_{i,\mu}^{(1)} \zeta_{i,\mu}^{(2)}. \qquad (3)$$

Their Fourier transforms,

$$\hat{q}_{\mu,\nu}(\vec{k}) = \sum_{i=1}^{N} \frac{q_{\mu,\nu}(\vec{r}_i) e^{i\vec{k}\cdot\vec{r}_i}}{L^3}, \qquad \hat{\kappa}_{\mu}(\vec{k}) = \sum_{i=1}^{N} \frac{\kappa_{i,\mu} e^{i\vec{k}\cdot\vec{r}_i}}{L^3}, \qquad (4)$$

yield the spin-glass (SG) wave vector dependent susceptibility and the chiral glass (CG) one:

$$\frac{\chi_{SG}(\vec{k})}{L^3} = \sum_{\mu,\nu} \overline{\langle |\hat{q}_{\mu,\nu}(\vec{k})|^2 \rangle_J}, \qquad \frac{\chi_{CG}^{\mu}(\vec{k})}{L^3} = \overline{\langle |\hat{\kappa}_{\mu}(\vec{k})|^2 \rangle_J}. \qquad (5)$$

Both for the SG and the CG case, we have [20]:

$$\xi_L = \frac{1}{2\sin(k_{min}/2)} \left(\frac{\chi(\vec{0})}{\chi(\vec{k}_{min})} - 1 \right)^{1/2}, \qquad (6)$$

where $\vec{k}_{min} = (2\pi/L, 0, 0)$ or permutations. One has $\xi_{CG}^{\perp}$ or $\xi_{CG}^{\parallel}$ for $\hat{e}_\mu \cdot \vec{k}_{min} = 0$ or $2\pi/L$, respectively [15]. Rotational invariance at T_c implies $\xi_{CG}^{\perp} = \xi_{CG}^{\parallel}$ for large L.

Model (1) was simulated with a mixture of heat bath and (microcanonical) overrelaxation taken from lattice QCD [21], but also effective for frustrated spin models [23]. We straightforwardly modified the implementation for $J_{ij} = 1$ in [5]. The elementary Monte Carlo step (EMCS) consists on a sequential heat bath sweep, followed by (the integer part of) $5L/4$ *sequential* overrelaxation sweeps, to let the microcanonical wave run over the system. Overrelaxation evolves chirality fast (in $D = 1$ it inverts the local chirality). One heat bath update is roughly as CPU time consuming as 7 overrelaxations. The merits of the mixed algorithm can be assessed from Fig. 1 (standard parallel tempering reached only $L = 12$ for the same model [15]). Overrelaxation may be combined with parallel tempering, but this is unnecessary at T_c. Lattices $L = 4, 6, 8, 12, 16, 24$, and 32 were simulated close to $T_c \approx 0.16(2)$ [13,15] (see Table I). We extrapolate to nearby temperatures using bias-corrected [24] data reweighting [25].

Thermalization is a major issue in SG simulations. Our thermalization tests included the by now standard $\log_2$ data binning (i.e., average over all samples the second half of the generated data, and compare this average with that of the second fourth of the Monte Carlo history, the average over the second eighth, and so on), finding compatibility for the last three bins. Another strong thermalization test is the consistency of the reweighting extrapolation [25]. As Fig. 3 shows, the reweighting extrapolation is satisfactory for our data. It is a nice check, because simulations at different T are completely independent.
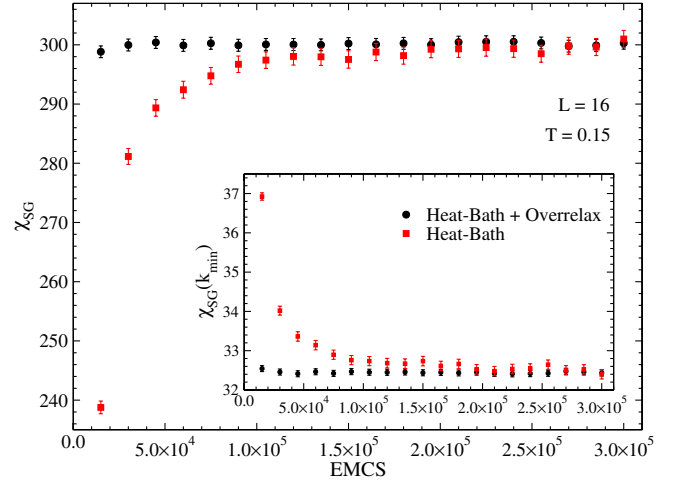

FIG. 1 (color online). Comparison of heat bath vs heat bath plus overrelaxation evolution of $\chi_{SG}(\vec{0})$ [$\chi_{SG}(\vec{k}_{min})$ in the inset] from a hot start (EMCS: either 1 heat bath step followed by 20 overrelaxation sweeps or 4 heat bath sweeps). Points in the plot are the average over 2500 samples of 15 000 successive EMCS.

We use the quotients FSS method [4]. The used scaling variable is ξ_L/L [4,6], rather than the unknown L/ξ_∞ or $(T - T_c)L^{1/\nu}$. For an observable O, diverging in the large L limit as $\langle \bar{O} \rangle_{J,L=\infty} \propto |T - T_c|^{x_O}$, we compare $\langle \bar{O} \rangle_J$ in lattices L_1 and L_2, at the crossing temperature T^{L_1,L_2} such that $\xi_{L_1}(T^{L_1,L_2})/L_1 = \xi_{L_2}(T^{L_1,L_2})/L_2$:

$$\frac{\overline{\langle O_{L_2}(T^{L_1,L_2}) \rangle_J}}{\overline{\langle O_{L_1}(T^{L_1,L_2}) \rangle_J}} = \left(\frac{L_2}{L_1} \right)^{x_O/\nu} + \ldots, \qquad (7)$$

where ν is the correlation length critical exponent (the dots stand for scaling corrections [5]). The advantages of Eq. (7) are many [2,4,7,24]. It is easy to use. Arbitrary choices on the temperature range are avoided. The statistical error estimation is crystal clear. One directly observes scaling corrections by increasing L_1 and L_2.

Should T^{L_1,L_2} be obtained from $\xi_{L,CG}$ or from $\xi_{L,SG}$? There is a consensus on the divergence of ξ_{CG} at T_c, while

TABLE I. Details of simulation. For each lattice size, we give the studied temperatures, the number of simulated samples (in the same order), and the number of elementary Monte Carlo steps per sample. In each sample we took 10^5 measurements, excepting for $L = 32$ (20 000 measurements).

L	4	6	8	12	16	24	32
T	0.15	0.15	0.15	0.150	0.150	0.146	0.145
	0.16	0.16	0.155	0.155	0.156	0.150	0.147
			0.160	0.160	0.160	0.155	0.150
$N_{samples}$ ($\times 10^3$)	2	4	2	3	2.5	2	1
	2	6	2	2.4	2.5	1.3	1
			2	3	2	2	2
EMCS $\times 10^5$	1	1	1	2	3	16	40

TABLE II. Critical exponents from Eq. (7) ($T^{L_1, L2}$ from $\xi_{L,\mathrm{CG}}^{\parallel}$). The O were: ξ_{SG} (ϕ: $\xi_{\mathrm{SG}} \sim L^{\phi}$), $\partial_T \xi_L / L$ ($1/\nu$), and χ (γ/ν). The $L_1 = 24$, $L_2 = 32$ crossing is unclear (Fig. 4), so we quote results at $T^{L_1, L_2} = 0.146$ (A) and 0.145 (B).

L_1	L_2	ϕ	$1/\nu_{\mathrm{SG}}$	$1/\nu_{\mathrm{CG}}$	$\gamma_{\mathrm{SG}}/\nu_{\mathrm{SG}}$	$\gamma_{\mathrm{CG}}/\nu_{\mathrm{CG}}$
4	8	1.047(5)	1.278(10)	1.077(20)	2.117(7)	1.061(10)
6	12	1.057(3)	1.223(10)	0.761(12)	2.056(5)	0.628(11)
8	16	1.013(4)	0.989(10)	0.722(12)	2.008(8)	0.738(18)
12	24	0.939(4)	0.71(17)	0.66(11)	1.954(9)	0.925(22)
16	24	0.917(5)	0.68(11)	0.67(12)	1.943(15)	1.02(4)
16	32	0.908(5)	0.72(20)	0.73(11)	1.945(13)	1.130(29)
24	32^A	0.88(2)	0.60(10)	0.64(12)	1.93(2)	1.26(7)
24	32^B	0.91(2)	0.56(12)	0.51(13)	1.96(4)	1.36(11)

that of ξ_{SG} is controversial [14,15]. Moreover, $\xi_{L,\mathrm{CG}}$ suffers smaller scaling corrections (Fig. 4). So, the results in Table II were obtained with $\xi_{L,\mathrm{CG}}$. As for $\xi_{L,\mathrm{SG}}$, we treat it here as an observable scaling as L^{ϕ}. Some groups [15–17] expect $\phi = 1$, while others [13,14] believe that $\phi = 0$.

Several features are salient in Table II. (i) Once we neglect $L = 4$, the L evolution of our estimates is monotonic with increasing L_1 and L_2 (we agree with Refs. [14,15] within their L window). (ii) The $1/\nu$ from $\partial_T \xi_{\mathrm{SG}}$ and $\partial_T \xi_{\mathrm{CG}}$ is compatible for $L \geq 12$. (iii) When L_1 and L_2 increases, $1/\nu$ systematically decreases (in a Kosterlitz-Thouless scenario it tends to zero). (iv) Exponent γ_{SG}/ν stabilizes for $L \geq 12$ in a typical $D = 3$ value [4], hence:

$$\chi_{\mathrm{SG}} \propto \xi_{\mathrm{CG}}^{1.93 \pm 0.02}. \tag{8}$$

The scenario of Refs. [13,14], where ξ_{CG} diverges at T_c, while ξ_{SG} (and then χ_{SG}) does not, becomes untenable.

At criticality (Table II), ξ_{SG} scales as $L^{0.9}$ rather than L^1, immediately suggesting the presence of logarithmic corrections to scaling. Without analytical guidance, the detailed numerical study of logarithmic scaling corrections [24] is out of reach. Thus, we borrow the leading scaling corrections from the $D = 2$ XY model [26] (f_{ξ} is a smooth scaling function, while A is a scaling amplitude):

$$\frac{\xi_{L,\mathrm{SG}}}{L} = f_{\xi}(\xi_{L,\mathrm{CG}}/L)\left(1 + \frac{A}{\log L} + \dots\right). \tag{9}$$

Indeed (see Fig. 2), Eq. (9) accounts for the $L^{0.9}$ scaling ($A = 1.3$, roughly 4 times that of the 2D-XY model [26]). One also expects [26] multiplicative logarithms in Eq. (8). Note, however, that Eq. (9) works in a limited range of L for any system barely above its lower critical dimension since it is the $\omega \to 0$ limit of the standard leading correction to scaling, $L^{-\omega}$ [5] (e.g. the $2 + \epsilon$ expansion [27] yields $\omega \approx \epsilon$ for the Heisenberg ferromagnet, whose lower critical dimension is two).

We now study ξ_{SG}/L as a function of temperature (Fig. 3). If we do not correct for scaling corrections
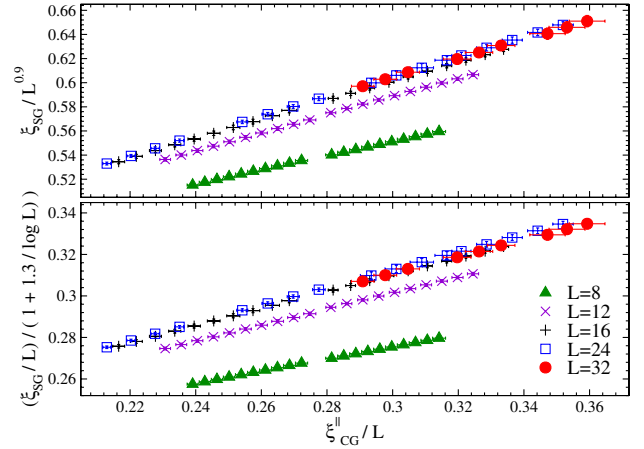

FIG. 2 (color online). Top: For our largest systems ξ_{SG} scales as $L^{0.9}$, using ξ_{CG}/L as scaling variable. Bottom: The results in the upper part may be interpreted as the logarithmic corrections to scaling in Eq. (9), particularly for $L > 12$.

(Fig. 3, top), indeed all crossings are in the rather large range $T_c = 0.16(2)$ [13,15]. However, we observe a net shift of the crossings to lower T when the system sizes grow, (for $L = 24$ and $L = 32$ a crossing is not found on the simulated T range). Yet, in Fig. 3, bottom, dividing out the logarithm scaling corrections in Eq. (9), the curves for the largest systems merge around $T = 0.146$, as expected for a Kosterlitz-Thouless transition (see, e.g., Ref. [2]).

For the sake of completeness, let us consider our data for $\xi_{L,\mathrm{SG}}$ under the spin-chirality decoupling assumption. In this scenario, $\xi_{\infty,\mathrm{SG}}$ diverges at $T = 0$, as $\xi_{\infty,\mathrm{SG}} = A/T^{\nu^*}$ ($\nu^* = 2.2$, according to [14]). FSS [5] predicts that $\xi_{L,\mathrm{SG}}/L$ is a smooth function of $L/\xi_{\infty,\mathrm{SG}}$. Take now, from Fig. 3, top, the temperature where $\xi_{L,\mathrm{SG}}/L$ reaches (say) 0.44 for $L = 24$ and $L = 32$, namely, $T_{24} \approx 0.1508$
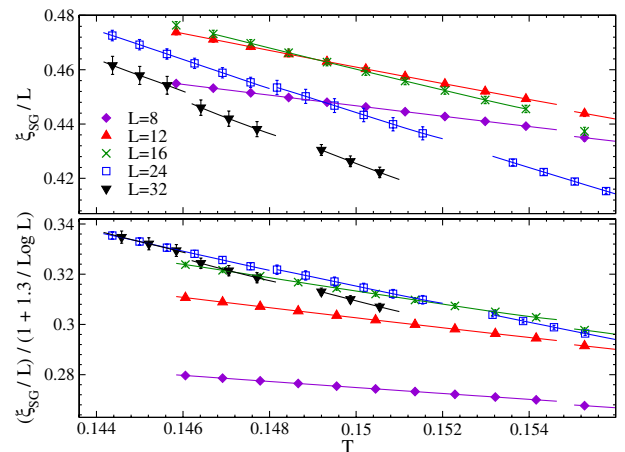

FIG. 3 (color online). Top: ξ_{SG} in units of L, versus T, for several lattice sizes. Lines join data obtained from a single simulation [25] (all simulations independent). For the sake of clarity we only represent data for $L \geq 8$. Bottom: as top, correcting the suspected logarithmic corrections, Eq. (9).
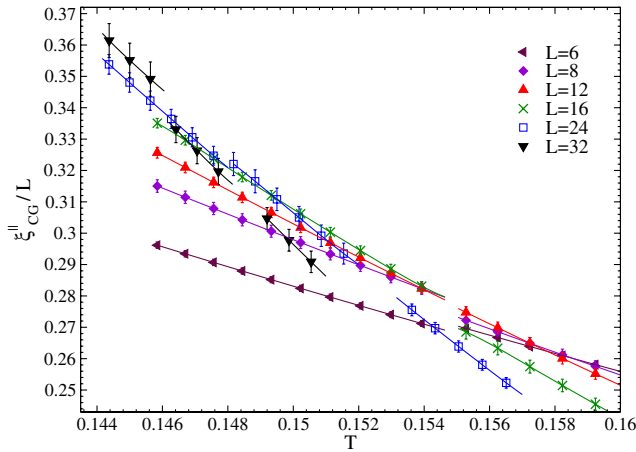
FIG. 4 (color online).   Parallel chiral correlation length in units of L, as a function of T, for several lattice sizes.

and $T_{32} \approx 0.1474$. In other words, $\xi_{\infty,\mathrm{SG}}$ increases a factor $32/24 \approx 1.33$, while the temperature merely decreases by 2%. Matching this with an algebraic divergence at $T = 0$, the nonsensical result $\nu^* \approx 12$ is obtained.

Consider now $\xi_{\mathrm{CG}}^{\parallel}/L$, shown in Fig. 4. Although less than for ξ_{SG}, the crossings shift to lower T for larger L. For $L = 8$, 12 and 16 we resolve a crossing at $T \approx 0.155$. For $L \geq 16$ the curves merge at $T \approx 0.147$, suggesting again a Kosterlitz-Thouless scaling, but with smaller scaling corrections. The $L = 32$ data at low T are compatible with, but above, the $L = 24$ data. We suspect a statistical fluctuation (the three $L = 32$ simulations are independent), but a crossing may not be discarded.

In summary, we have shown that the Heisenberg spin glass undergoes a spin-glass transition in $D = 3$, by means of Monte Carlo simulation and FSS analysis [2,4,5]. We have adapted a lattice gauge theory algorithm [21], that thermalizes $L = 32$ systems, well beyond any previous spin-glass simulation in $D = 3$. Furthermore, a large number of samples were studied in Marenostrum. For studies in the low temperature phase, we suggest combining our algorithm with parallel tempering. The large range of system sizes studied allows us to conclude that, at criticality, the spin-glass susceptibility scales with the *chiral* correlation length, Eq. (8). Therefore, a single phase transition is present in this problem: spin-chirality decoupling is ruled out. We observe logarithmic corrections to scaling, explaining why previous investigations [9–17] were inconclusive. Our results are compatible with Kosterlitz-Thouless scaling, but they are typical as well of a system with a lower critical dimension barely smaller than 3.

[1] See e.g. *Spin Glasses and Random Fields*, edited by A. P. Young (World Scientific, Singapore, 1997); M. Mézard, G. Parisi, and M. A. Virasoro, *Spin-Glass Theory and Beyond* (World Scientific, Singapore, 1987).

[2] H. G. Ballesteros *et al.*, Phys. Rev. B **62**, 14 237 (2000).

[3] M. Palassini and S. Caracciolo, Phys. Rev. Lett. **82**, 5128 (1999).

[4] H. G. Ballesteros *et al.*, Phys. Lett. B **378**, 207 (1996); **387**, 125 (1996); Nucl. Phys. **B483**, 707 (1997).

[5] See, e.g., D. Amit and V. Martin-Mayor, *Field Theory, the Renormalization Group and Critical Phenomena* (World-Scientific, Singapore, 2005), 3rd ed.

[6] S. Caracciolo *et al.*, Phys. Rev. Lett. **74**, 2969 (1995).

[7] T. Jörg, Phys. Rev. B **73**, 224431 (2006).

[8] H. G. Katzgraber, M. Körner, and A. P. Young, Phys. Rev. B **73**, 224432 (2006).

[9] W. L. McMillan, Phys. Rev. B **31**, 342 (1985); J. A. Olive, A. P. Young, and D. Sherrington, *ibid.* **34**, 6341 (1986); B. M. Morris *et al.*, J. Phys. C **19**, 1157 (1986).

[10] F. Matsubara, T. Iyota, and S. Inawashiro, Phys. Rev. Lett. **67**, 1458 (1991).

[11] D. Imagawa and H. Kawamura, Phys. Rev. Lett. **92**, 077204 (2004).

[12] A. Mauger *et al.*, Phys. Rev. B **41**, 4587 (1990).

[13] H. Kawamura, Phys. Rev. Lett. **80**, 5421 (1998); K. Hukushima and H. Kawamura, Phys. Rev. E **61**, R1008 (2000).

[14] K. Hukushima and H. Kawamura, Phys. Rev. B **72**, 144416 (2005).

[15] L. W. Lee and A. P. Young, Phys. Rev. Lett. **90**, 227203 (2003).

[16] F. Matsubara, T. Shirakura, and S. Endoh, Phys. Rev. B **64**, 092412 (2001); T. Nakamura and S. Endoh, J. Phys. Soc. Jpn. **71**, 2113 (2002).

[17] M. Picco and F. Ritort, Phys. Rev. B **71**, 100406 (2005).

[18] F. Bert *et al.*, Phys. Rev. Lett. **92**, 167203 (2004).

[19] D. Petit, L. Fruchter, and I. A. Campbell, Phys. Rev. Lett. **83**, 5130 (1999); **88**, 207206 (2002).

[20] F. Cooper, B. Freedman, and D. Preston, Nucl. Phys. **B210**, 210 (1982).

[21] F. R. Brown and T. J. Woch, Phys. Rev. Lett. **58**, 2394 (1987).

[22] J. M. Kosterlitz and D. J. Thouless, J. Phys. C **6**, 1181 (1973).

[23] J. L. Alonso *et al.*, Phys. Rev. B **53**, 2537 (1996); E. Marinari, V. Martin-Mayor, and A. Pagnani, *ibid.* **62**, 4999 (2000).

[24] H. G. Ballesteros *et al.*, Nucl. Phys. **B512**, 681 (1998).

[25] M. Falcioni *et al.*, Phys. Lett. B **108**, 331 (1982); A. M. Ferrenberg and R. H. Swendsen, Phys. Rev. Lett. **61**, 2635 (1988).

[26] M. Hasenbusch, J. Phys. A **38**, 5869 (2005).

[27] A. M. Polyakov, Phys. Lett. B **59**, 79 (1975); E. Brèzin and J. Zinn-Justin, Phys. Rev. B **14**, 3110 (1976).